

Ion-Exchange Calculations Using Spreadsheets

M. Carmona, J.F. Rodríguez and A. Durán*

Department of Chemical Engineering, Facultad de Ciencias Químicas, Universidad de Castilla-La Mancha, CIUDAD REAL 13004 SPAIN, aduran@inqu-cr.uclm.es

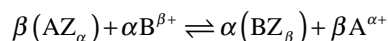
Abstract: A simple set of calculations using a Microsoft Excel spreadsheet can help students determine ion-exchange equilibrium parameters, essential for the design of industrial equipment. Equilibrium parameters are evaluated from experimental isotherms obtained from different zeolites using the action-law model by means of nonlinear curve fitting (Marquardt method). Students will be able to discriminate between ideal and nonideal systems by observation of activity coefficients. The possibility of using the spreadsheet with different types of ion-exchange materials is also validated by comparing the model results with experimental data from papers available in the recent literature. Although the laboratory experience is laborious, it is very satisfactory.

Introduction

Mathematical tools in the chemistry and chemical engineering curriculum need to be introduced early in a student's matriculation. These tools can be used to teach students about the suitability of scientific models and to help them understand the practical applicability of such models. Computer concepts should be included in the curriculum because students must be prepared to use computers throughout their academic and professional lives. Spreadsheet applications are advantageous for teaching purposes because they can be used by students with little computer experience, but with time to learn spreadsheet skills [1].

There is, as well, a need to present ion-exchange fundamentals in a suitable form for chemical engineering process design and development. The major industrial application of ion exchange is water treatment (i. e., the demineralization of boiler feed water, condensate polishing, and the production of ultrapure water for the microelectronic industry). These applications require the design and operation of large-scale fixed-bed ion-exchange columns. For this purpose, all two-phase solid/liquid mass-transfer processes require an established equilibrium theory and a coherent rate theory coupled to a hydrodynamic model in order to facilitate rational design.

The electroneutrality-restricted exchange of two ions has similarities with a chemical reaction. Consider the exchange of cations A and B using a cation-exchange resin with the resin initially containing only B ions, the A ions being in the external solution. The exchange process may be represented by the general equation



The classical way of teaching the equilibrium behavior of ion exchangers is based on the law of mass action. The assumption of ideal behavior in the liquid and solid phases leads to a nonrigorous approach where a separation factor is calculated from the concentration of the species in each phase. If a more rigorous thermodynamic treatment is developed, however, the equilibrium constant has to be calculated from the activities of the ions, which requires the estimation of the

activity coefficients in both phases. To this end, a number of generally accepted equations for the liquid phase can be used, for instance Pitzer [2], Debye–Hückel [3] or Meissner–Kusik [4]. In these equations the parameters for each salt or solution can be obtained from the literature; thus, it is not usually necessary to evaluate any of them. Still, there is no theoretical correlation for obtaining the solid-phase activity coefficients of the individual ions. They have to be evaluated using analogous methods to those proposed for liquid/vapor equilibrium. The equations used to calculate activity coefficients based on the Wilson model include two adjustable parameters that, although depending on the characteristics of the system, cannot be predicted on a theoretical basis. In practice, the evaluation of these parameters, which are included in a nonlinear set of equations, requires using a nonlinear least-squares regression method [5]. In this work, a sequence of calculations has been performed in a Microsoft Excel spreadsheet to solve this problem.

The goals of this article are:

- to emphasize the capability of spreadsheets for solving specific common problems in chemistry and chemical engineering,
- to perform an elementary sequence of calculations in an Excel spreadsheet correlating experimental equilibrium data using nonlinear curve fitting (Marquardt method),
- to use this model to understand how activity coefficients correct deviations from ideal equilibrium behavior.

Results and Discussion

How the Spreadsheet Works. The instructor should have previously explained ion-exchange theory in the classroom so that the equilibrium equations and activity coefficients in both phases, shown in Table 1 (overbars refers to the solid phase), are known. The activity coefficients in the liquid phase are calculated from Meissner–Kusik equations. The solid-phase activity coefficients are obtained using the Wilson equations. To solve this nonlinear system, a sequence of calculations (Figure 1) has been performed using a Microsoft Excel 7.0 spreadsheet (provided in the supporting material). The $\Lambda_{BA, \text{new}}$

Table 1. Ion-exchange equations that determine the equilibrium and activity coefficients

Ion-exchange equilibrium	
$\beta (AZ_\alpha) + \alpha B^{\beta+} \rightleftharpoons \alpha (BZ_\beta) + \beta A^{\alpha+}$	(1)
$K_{AB}(T) \equiv \frac{\overline{a_A^\beta} a_B^\alpha}{\overline{a_B^\alpha} a_A^\beta}$	(2)
$K_{AB}(T) \equiv \frac{[\overline{X_B} \gamma_B]^\alpha [(1 - X_B) C_T \gamma_{ACl_\alpha}^{(\alpha+1)}]^\beta}{[(1 - \overline{X_B}) \gamma_A]^\beta [X_B C_T \gamma_{BCl_\beta}^{(\beta+1)}]^\alpha}$	(3)
$\overline{X}_i \equiv \frac{n_i}{n_\infty}$	(4a)
$X_i \equiv \frac{C_i}{C_T}$	(4b)
Activity coefficients	
Liquid phase (from references 4–7):	
$\log \gamma_{AD_\alpha} \equiv \frac{\alpha}{2} \left[\frac{\log \gamma_{AD_\alpha}^0}{\alpha} (Y_D + x_{A'}) + \frac{x_{B'}}{\beta} \log \gamma_{BD_\beta}^0 \right]$	(5a)
$\log \gamma_{BD_\beta} \equiv \frac{\beta}{2} \left[\frac{\log \gamma_{BD_\beta}^0}{\alpha} (Y_D + x_{B'}) + \frac{x_{A'}}{\alpha} \log \gamma_{AD_\alpha}^0 \right]$	(5b)
$x_{A'} = \frac{m_A \alpha^2}{m_A \alpha^2 + m_B \beta^2}$	(6a)
$x_{B'} = \frac{m_B \beta^2}{m_A \alpha^2 + m_B \beta^2}$	(6b)
$\log \gamma_{AD_\alpha}^0 = \frac{-A\alpha\mu^{0.5}}{(1 + d_{AD_\alpha} B\mu^{0.5})} - \left(\frac{1}{2.303v} \right) k.h_{\epsilon_{AD_\alpha}}^* (a_b - 1.0) - \log [1 + 1.018(v - k.h_{\epsilon_{AD_\alpha}}^* a_b)m_{AD_\alpha}]$	(7a)
$\log \gamma_{BD_\beta}^0 = \frac{-A\beta\mu^{0.5}}{(1 + d_{BD_\beta} B\mu^{0.5})} - \left(\frac{1}{2.303v} \right) k.h_{\epsilon_{BD_\beta}}^* (a_b - 1.0) - \log [1 + 1.018(v - k.h_{\epsilon_{BD_\beta}}^* a_b)m_{BD_\beta}]$	(7b)
$\log a_b = -4.02091 \times 10^{-3} \theta - 0.2152 \times 10^{-5} \theta^2 + 0.359 \times 10^{-7} \theta^3 + 0.212 \times 10^{-9} \theta^4 + 0.095 \times 10^{-11} \theta^5 + \dots$	(8)
$\theta = km_{AD_\alpha}$	(9)
$\mu = \frac{1}{2} (m_A \alpha^2 + m_B \beta^2 + m_D 1^2)$	(10)
Solid phase (Wilson equations)	
$\ln \overline{\gamma}_A \equiv 1 - \ln (\overline{X}_A + \overline{X}_B \Lambda_{AB}) - \frac{\overline{X}_A}{X_A + X_B \Lambda_{AB}} - \frac{\overline{X}_B \Lambda_{BA}}{X_B + X_A \Lambda_{BA}}$	(11a)
$\ln \overline{\gamma}_B \equiv 1 - \ln (\overline{X}_B + \overline{X}_A \Lambda_{BA}) - \frac{\overline{X}_B}{X_B + X_A \Lambda_{BA}} - \frac{\overline{X}_A \Lambda_{AB}}{X_A + X_B \Lambda_{AB}}$	(11b)

and $\lambda_{\text{Marquardt}}$ must be changed to a low value (e.g., 10) to obtain a better fit. Equations used to fit the model are given in Table 2. The scheme in Figure 1 can be condensed to the following steps:

- input known data for each electrolyte (C_T , \overline{X}_B^* , \overline{Y}^* , B , A , k , h_e , d),
- initial values of unknown parameters (K_{AB} , Λ_{AB} , Λ_{BA}), calculation of activity coefficients in both phases (simple application of equations 5–11 in Table 1),
- development of Marquardt method (equations 12–20 in Table 2),

d) calculation of $(\mathbf{b}_{\text{new}} - \mathbf{b}_{\text{old}})$ to test the accuracy of the method,

e) calculation of new iterative values if necessary.

A screen from the spreadsheet is shown in Figure 2.

The use of the built-in solver helps in the resolution of the problem, but some restrictions have to be made because $T \ln \overline{\gamma}_i^\alpha$ is constant, which requires the Wilson parameters to be positive.

The program usually allows the equilibrium parameters to be determined in one or two steps. A critical point in nonlinear fits is the initial choice of parameter values. If the initial values

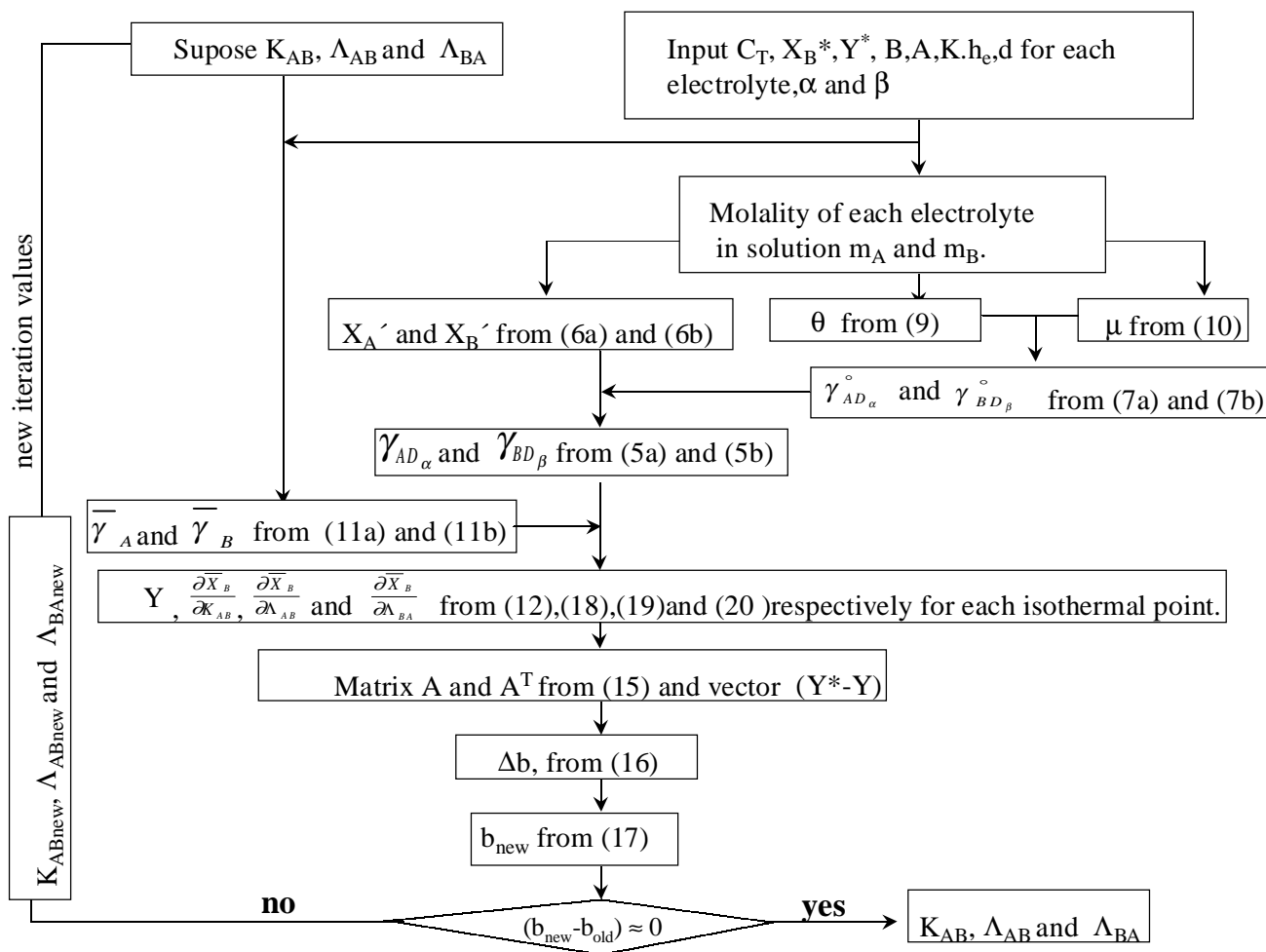


Figure 1. Sequence of calculations.

Table 2. Equations Used in the Fitting

From (3) and (11):

$$Y = \overline{X}_B \left[\frac{K_{AB} * [X_B * C_T * \gamma_{BD\beta}^{\beta+1}]^\alpha (1 - \overline{X}_B)^\beta e^{\left(\frac{\beta * \overline{X}_A}{X_A + \overline{X}_B * \Lambda_{AB}} - \frac{\beta * \overline{X}_B * \Lambda_{BA}}{X_B + \overline{X}_A * \Lambda_{BA}} \right)}}{\left(\overline{X}_A + \overline{X}_B * \Lambda_{AB} \right)^\beta} \right]^{1/\alpha} \quad (12)$$

$$\left[(1 - X_B) C_T \gamma_{AD\alpha}^{\alpha+1} \right]^\beta e^{\left(\frac{\alpha * \overline{X}_B}{X_B + \overline{X}_A * \Lambda_{BA}} - \frac{\alpha * \overline{X}_A * \Lambda_{AB}}{X_A + \overline{X}_B * \Lambda_{AB}} \right)} \left(\overline{X}_B + \overline{X}_A * \Lambda_{BA} \right)^\alpha$$

Marquardt method (Reference 5)

$$Y(x, \mathbf{b} + \Delta \mathbf{b}) = Y(x, \mathbf{b}) + \frac{\partial Y}{\partial \mathbf{b}} \Delta \mathbf{b} \quad (13)$$

$$\phi = (\mathbf{Y}^* - \mathbf{Y} - \mathbf{A} \Delta \mathbf{b})^T (\mathbf{Y}^* - \mathbf{Y} - \mathbf{A} \Delta \mathbf{b}) \quad (14)$$

$$\mathbf{A} = \begin{bmatrix} \frac{\partial Y_1}{\partial b_1} & \dots & \frac{\partial Y_1}{\partial b_k} \\ \dots & \dots & \dots \\ \frac{\partial Y_n}{\partial b_1} & \dots & \frac{\partial Y_n}{\partial b_k} \end{bmatrix} \quad (15)$$

$$\Delta \mathbf{b} = (\mathbf{A}^T \mathbf{A} + \lambda \mathbf{I})^{-1} \mathbf{A}^T (\mathbf{Y}^* - \mathbf{Y}) \quad (16)$$

$$\mathbf{b}_{new} = \mathbf{b}_{old} + \Delta \mathbf{b} \quad (17)$$

Derivatives From (14) (Table 2 cont.)

$$\frac{\partial Y}{\partial b_1} = \frac{\partial \bar{X}_B}{\partial K_{AB}} = \frac{1}{\alpha K_{AB}} \times \left[\frac{K_{AB} * [X_B * C_T * \gamma_{BD\beta}]^\alpha (1 - \bar{X}_B)^\beta * e^{\left(\frac{\beta - \beta \bar{X}_A}{\bar{X}_A + \bar{X}_B * \Lambda_{AB}} - \frac{\beta * \bar{X}_B * \Lambda_{BA}}{\bar{X}_B + \bar{X}_A * \Lambda_{BA}} \right)}}{\left(\bar{X}_A + \bar{X}_B * \Lambda_{AB} \right)^\beta} \right]^{1/\alpha} \quad (18)$$

$$\frac{\partial Y}{\partial b_2} = \frac{\partial \bar{X}_B}{\partial \Lambda_{AB}} = \frac{1}{K_{AB}} (1 - \bar{X}_B)^\beta X_B C_T \gamma_{BD\beta}^{(\beta+1)} (\bar{X}_B + \bar{X}_A \Lambda_{BA}) e^{\left[\frac{\beta - \alpha}{\alpha} \frac{\alpha \bar{X}_B - \beta \bar{X}_B \Lambda_{BA} + \bar{X}_A (\alpha \Lambda_{AB} - \beta)}{\alpha \bar{X}_B + \alpha \bar{X}_A \Lambda_{BA} + \alpha (\bar{X}_A + \bar{X}_B \Lambda_{AB})} \right]} \times \left[(1 - \bar{X}_B) C_T \gamma_{AD\alpha}^{(\alpha+1)} \right]^\beta * (\bar{X}_A + \bar{X}_B \Lambda_{AB})^\beta \quad (19)$$

$$\left[\frac{(\alpha \bar{X}_A + \alpha \bar{X}_B \Lambda_{AB}) \alpha \bar{X}_A - (\alpha \bar{X}_A \Lambda_{AB} + \beta \bar{X}_A) * \alpha \bar{X}_B}{(\alpha \bar{X}_A + \alpha \bar{X}_B \Lambda_{AB})^2} - \frac{\beta \bar{X}_B}{(\bar{X}_A + \bar{X}_B \Lambda_{AB}) \alpha} \right] \quad (20)$$

$$\frac{\partial Y}{\partial b_3} = \frac{\partial \bar{X}_B}{\partial \Lambda_{BA}} = \frac{1}{K_{AB}} (1 - \bar{X}_B)^\beta X_B C_T \gamma_{BD\beta}^{(\beta+1)} e^{\left[\frac{\beta - \alpha}{\alpha} \frac{\alpha \bar{X}_A \Lambda_{AB} - \beta \bar{X}_A}{\bar{X}_A + \bar{X}_B \Lambda_{AB}} + \frac{\alpha \bar{X}_B - \beta \bar{X}_B \Lambda_{BA}}{\alpha \bar{X}_B + \alpha \bar{X}_A \Lambda_{BA}} \right]} \times \left[(1 - \bar{X}_B) C_T \gamma_{AD\alpha}^{(\alpha+1)} \right]^\beta (\bar{X}_A + \bar{X}_B \Lambda_{AB})^\beta \quad (20)$$

$$\left[\frac{\beta \alpha \bar{X}_B (-1) (\bar{X}_B + \bar{X}_A \Lambda_{BA}) - (\alpha \bar{X}_B - \beta \bar{X}_B \Lambda_{BA}) * \alpha \bar{X}_A}{(\bar{X}_B + \bar{X}_A \Lambda_{BA})^2 \alpha^2} \right]$$

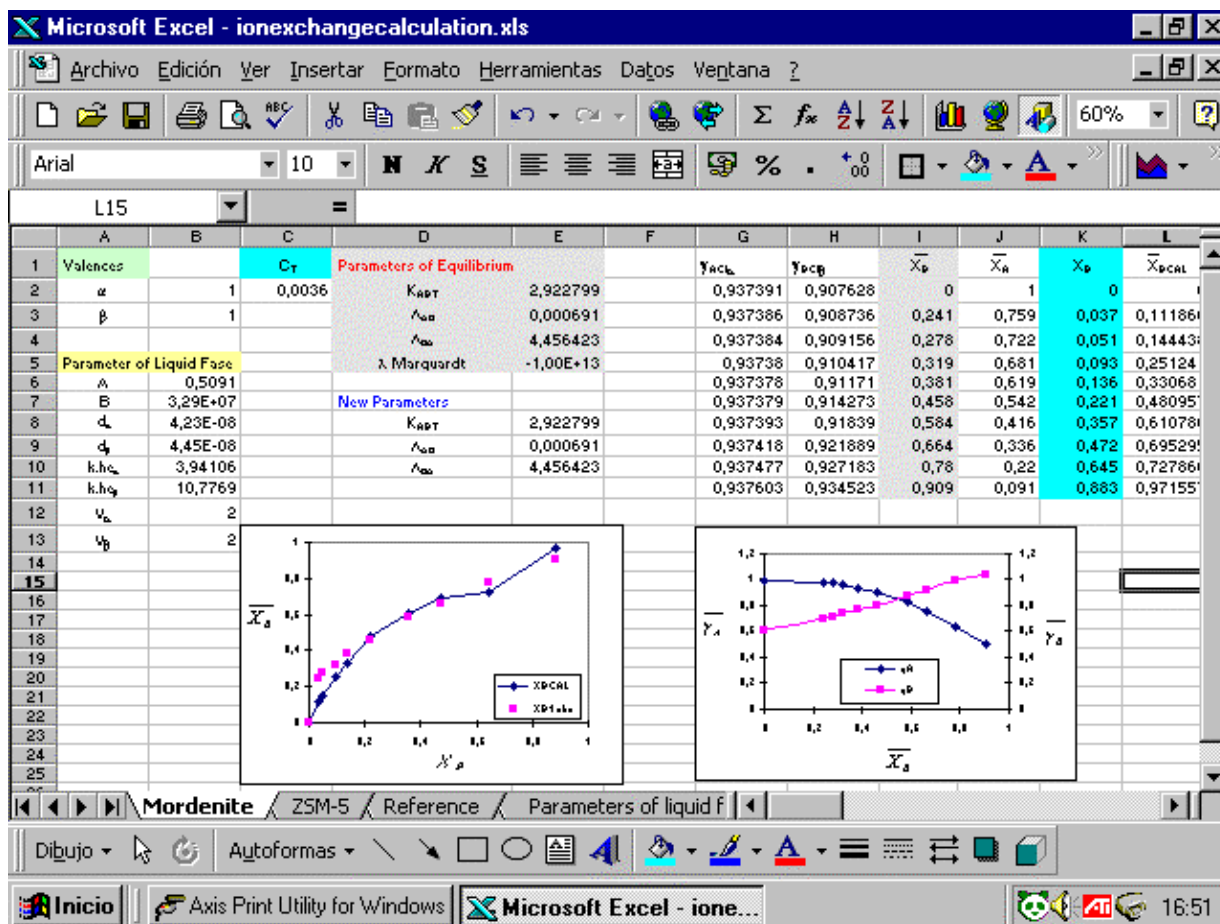


Figure 2. Appearance of the Spreadsheet Screen.

Table 3. Experimental Planning and Results (T = 298 K; C_T = 0.036 M)

Sample type	Sample weight (g)	Volume of 0.1 N HCl (ml)	[Na ⁺] meq/L	X _B	\overline{X}_B
ZSM-5	0.0362	50	0.704	0.804	0.976
	0.0645		1.225	0.673	0.95
	0.0898		1.617	0.550	0.905
	0.1344		2.213	0.385	0.827
	0.1803		2.595	0.278	0.723
	0.2281		2.847	0.209	0.627
	0.2698		3.034	0.157	0.565
	0.3161		3.165	0.120	0.503
	0.118		4.204	0.883	0.909
	0.401		12.762	0.645	0.780
Mordenite	0.701	50	18.999	0.472	0.664
	1.003		23.130	0.357	0.584
	1.500		28.043	0.221	0.458
	2.000		31.082	0.136	0.381
	2.505		32.627	0.093	0.319
	3.006		34.147	0.051	0.278
	3.512		34.659	0.037	0.241

Table 4. Constants Used in Equation 7a and b. Temperature 298K

System	A	B	k.h _e	d
HCl	0.5091	3.29 × 10 ⁷	3.94106	4.23 × 10 ⁻⁸

are far from the true ones, convergence may not be obtained. A good choice is to suppose both Λ_{AB} and Λ_{BA} equal 1. Also, the initial value of the $\lambda_{\text{Marquardt}}$ parameter is a determinant to obtaining a good fit. This value must be high in the first step (e.g., 10²⁰) to decrease the number of iterations required to reach convergence. If a second step is needed, the values proposed by the model should be used ($K_{AB,\text{new}}$, $\Lambda_{AB,\text{new}}$, and $\Lambda_{BA,\text{new}}$) and $\lambda_{\text{Marquardt}}$ must be changed to a low value (e.g., 10) to obtain a better fit.

This fit is very sensitive to erroneous data. If poor convergence with jumps in the fit parameters is obtained, experimental data should be re-acquired.

Obtaining and Interpreting Experimental Data. In order to obtain experimental equilibrium data with Mordenite and ZSM-5 zeolites that can be used to illustrate the model, a simple but effective experimental setup is needed. The necessary equipment and chemicals include:

- ten Pyrex-glass flasks (100 ml) with magnetic stirrers,
- one temperature-controlled thermostatic bath,
- 15 g of Na-Mordenite (Valfor C500-11, Si/Al=6.5, capacity = 1.83 meq/g supplied by PQ Corporation in Leiden, The Netherlands)
- 1.5 g of ZSM-5 (Si/Al = 20, capacity = 0.995 meq/g, synthesized using ethanol as template according to the method described by Uguina et al. [8]),
- 1000 ml of 0.1 N hydrochloric acid (prepared from HCl 35% wt, Panreac).

The flasks are filled with a preweighed amount of ion exchanger in its sodium form and a fixed volume of 0.1 N hydrochloric acid. They are sealed hermetically (all data are in Table 3). The flasks are then maintained at 298 K with vigorous stirring for three hours. Once equilibrium has been

reached, the ion exchanger is poured out and the ionic solutions are analyzed by atomic absorption spectroscopy (an accurate titration of the solution may also be used). The equilibrium composition in the solid phase is determined by mass balance. Results are shown in Table 3 to help in the execution of the experiments.

In order to apply the model to the computation of ion-exchange equilibrium parameters from experimental data obtained in the laboratory for Mordenite and ZSM-5 zeolites, the equations in Table 1 and 2 have to be written in terms of the actual ions (A = Na⁺, B = H⁺, D = Cl⁻).

The values of $k.h_e^*$ and d were obtained by nonlinear regression from the activity coefficients of the pure salt, γ_{D_B} , obtained from the literature [9]. (See Table 4 and the spreadsheet.) These values can be given to the students ad hoc to reduce the time employed in calculations and to keep their focus on the target problem. Debye-Hückel equations are generally better known by the students to calculate activity coefficients in electrolyte solutions. Although their application range is more limited (used only under 0.1 M), they are a simpler alternative method when dilute solutions are used.

Figure 3 shows the experimental equilibrium isotherms of both zeolites, together with the fits obtained from the Excel-based calculations. It can be seen that both isotherms are over the diagonal, illustrating the preference of the zeolites for the more highly

hydrated radius ion (H⁺). This is opposite to the behavior of some synthetic resins under the same conditions [6]. Equilibrium constants and binary Wilson parameters obtained from the fitting procedure are given in Table 5.

Deviations from Ideal Equilibrium Behavior. The spreadsheet program also allows the activity coefficients for both ions to be obtained. As an example, $\overline{\gamma}_H$ (hydrogen) is drawn versus \overline{X}_H in Figure 4 for both zeolites. Students must be told that ZSM-5 zeolite behaves as an ideal system, whereas Mordenite is a nonideal system because the activity coefficients in the resin phase are different from unity.

Comparison with Data in the Literature. The sequence of calculations described provides data that compares well with

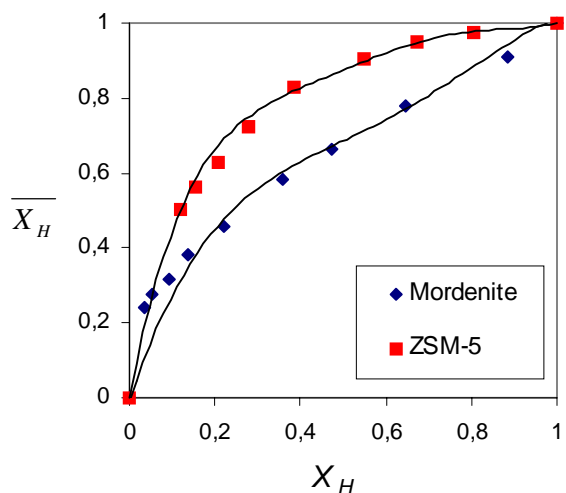


Figure 3. Equilibrium isotherms. Experimental data (■: ZSM-5; ◆: Mordenite) and best-fit of model (—). Conditions: $C_T = 0.036$ M, $T = 298$ K, $V = 50$ mL.

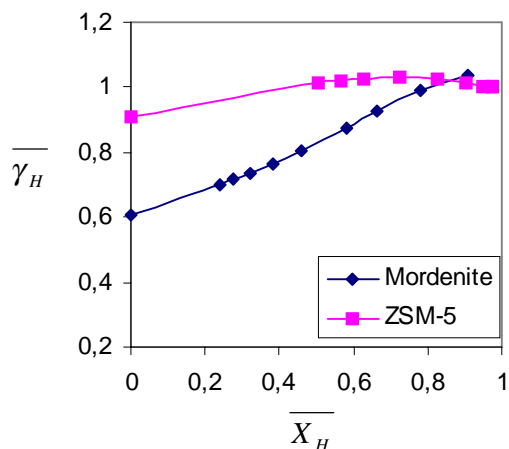


Figure 4. Activity coefficients (H^+) in ZSM-5 and Mordenite solid phases. Conditions: $C_T = 0.036$ M, $T = 298$ K, $V = 50$ mL.

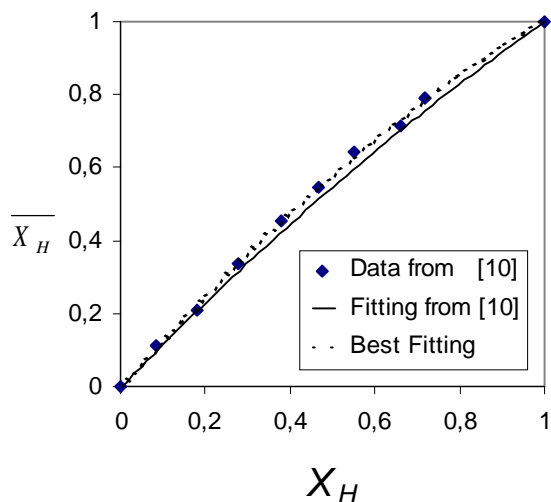


Figure 5. Equilibrium isotherms. Experimental data from reference 10 (◆), best fit from reference 10 (—), and best fit obtained with the set of calculations developed in Excel (.....). Conditions: $C_T = 0.1$ M, $T = 303$ K, $V = 500$ mL.

Table 5. Equilibrium Parameters for Mordenite/HCl and ZSM5/HCl (Conditions: $C_T = 0.036$ M, $T = 298$ K, $V = 50$ mL)

System	K_{AB}	Λ_{AB}	Λ_{BA}
Mordenite/HCl	2.928	0.0007	4.45664
ZSM5/HCl	8.072	0.1447	2.5831

Table 6. Data from Lucas et al. for ion-exchange of H^+ - Na^+ in Amberlite IR-120 resins [10] (Conditions: $C_T = 0.1$ M, $T = 303$ K, $V = 500$ mL)

X_H	\bar{X}_H	\bar{X}_H Fitting from [10]
0	0	0
0.085	0.113	0.122
0.182	0.211	0.259
0.278	0.335	0.379
0.379	0.453	0.495
0.468	0.545	0.593
0.551	0.645	0.646
0.660	0.713	0.827
0.718	0.792	0.787
1	1	1

Table 7. Some Typical Industrial Parameters in the Design of Ion-Exchangers

Parameter	Value
Bed height	0.6–3.6 (m)
Pressure drop	0.3–0.6 (m of water)
Liquid flow	4–40 (bed volumes per h)
Superficial velocity	30–60 ($m\ h^{-1}$) in water treatment
Regeneration period	15–60 (min) ¹

that published in the literature for ion exchange of H^+ and Na^+ in Amberlite IR-120 resins [10]. These data are summarized in Table 6. Our best-fit parameters, shown in Figure 5, are $K = 1.591$ (1.51), $\Lambda_{AB} = 0.999$ (1.0) and $\Lambda_{BA} = 1.017$ (1.0) (values in parenthesis were obtained by De Lucas et al. [10] assuming ideal behavior).

Accordingly, students can also use this spreadsheet to fit a nonlinear model to experimental equilibrium ion-exchange data from the literature.

Industrial Applications

The main industrial application of ion exchange is water treatment. The instructor should explain to the students in the classroom that any application, including the demineralization of boiler feed water and the production of ultrapure water, requires the design of large-scale fixed-bed ion-exchange columns based on the equilibrium and kinetic data of the system. Industrial use also requires regeneration of the ion exchanger. Some typical parameters for industrial ion-exchange equipment are summarized in Table 7.

Experience in Our Laboratory. Before the experiment is begun, the instructor must have explained the theoretical concepts of ion-exchange equilibrium in the classroom. This experiment should be made in two sessions. During the first session, experimental data are obtained. During the second session, the spreadsheet calculations are performed for these data and for data from the literature. Students also learn about deviations from ideal behavior. Although this experiment may seem easily doable by the students, the instructor must pay continuous attention, especially during the analysis or ion

concentration, the calculation of the equilibrium composition in the solid phase by mass balance, and while performing the least-squares fit using the spreadsheet. It is an intense task, but the final results are appreciated by the students.

Conclusion

Spreadsheet calculations have been applied to the evaluation of essential data for the design of a typical unit operation in chemical engineering. The speed of computation and ease of execution allow students to concentrate on the physical meaning of the parameters used in the process. The sequence of calculations developed in Excel is suitable for comparison to literature data, and they help to clarify the difference between the different solid phases (resins or zeolites). Results are obtainable for ideal and non-ideal systems.

Nomenclature

A: first derivative matrix or Jacobian matrix of **Y**
 \mathbf{A}^T : transpose of **A** matrix
A, **B**: Debye-Hückel parameters
 a_b : solvent activity, which can be calculated from [6]
 \bar{a}_i : molal activities of the ions in the solid
 a_i : molal activities of the ions in the external solution
b: vector of parameters
 C_i : ionic concentration of *i*
 C_T : total concentration in the solution.
d: equivalent diameter of ions in the salt.
D: co-ions of solution
I: identity matrix
 $k.h_e^*$: coordination number of ions in the salt.
k: cryoscopic constant
k: number of parameters
 K_{AB} : equilibrium constant
 m_A , m_B : molal concentrations of cations in the binary mixture
n: experimental observations
 n_i : meq. of *i*
 n_{∞} : total meq per gram of zeolite
T: absolute temperature
v: number of ions formed by dissociation of an electrolyte.
x: independent variable (liquid-phase concentration)
 x_A , x_B : ionic fraction of the cations in solution
 X_i : molar fractions of the ions in each phase (overbars refers to the solid phase)

\mathbf{X}_B^* : vector of the *n* experimental observations of the independent variable, X_{B_n}

Y*: vector of the *n* experimental observations of the dependent variable, \bar{X}_{B_n}

Y: vector of calculated values of the dependent variable

Y_D : ionic strength fraction of anion **D** referred to the total ionic strength of the anionic species

Greek

α , β : stoichiometric coefficients

γ : activity coefficients

γ_{AD_α} , γ_{BD_β} : activity coefficients in the liquid phase for the salt in solution

$\gamma_{AD_\alpha}^\circ$, $\gamma_{BD_\beta}^\circ$: activity coefficients of each pure at the same ionic total strength

$\lambda_{\text{Marquardt}}$: Marquardt parameter

Λ_{AB} , Λ_{BA} : Wilson equation parameters

μ : total ionic strength in the solution

ϕ : square residuals

θ : melting point decrease

References

1. Machuca, J. O. *J. Chem. Educ.* **1997**, 74(4), 448.
2. Shallcross, D. C.; Hermann, C. C.; McCoy, B. *J. Chem. Eng. Sci.* **1998**, 42(2), 279.
3. Allen, R. M.; Adisson, P. A.; Dechapunya, A. H. *Chem. Eng. J.* **1989**, 40, 151.
4. Meissner, H. P.; Kusik, C. L. Activity coefficients of strong electrolytes in multicomponent aqueous solutions. *AIChE J.* **1972**, 18(2), 294.
5. Contantinides, A. *Applied Numerical Methods with Personal Computers*; McGraw-Hill: New York, 1987; p 569.
6. De Lucas, A.; Zarca, J.; Cañizares, P. *Sep. Sci. Tech.* **1992**, 27(6), 823.
7. Klotz, I. M.; Rosenberg, R. M. *Termodinámica Química*. AC Libros Científicos y Técnicos: Madrid, 1977 p 413.
8. Uguina, M. A.; Lucas, A.; de Ruiz, F.; Serrano, D. *Ind. Eng. Chem. Res.*, **1995**, 34, 451.
9. Lide, D. R., Ed. *CRC Handbook of Chemistry and Physics*, 74th ed.; CRC Press: Boca Raton, FL, 1993-94, pp 5-92.
10. De Lucas, A.; Zarca, J.; Cañizares, P. *Int. Chem. Eng.* **1994**, 34(4), 486.